

High-resolution Imaging Optics Needing No Assembly-phase Optical Adjustments

The use of modern computer numerical control (CNC) machining tools have opened new possibilities for the optical and optomechanical designs. The fusion of optics and optomechanics has been earlier demonstrated by the integration of mirror optics directly to the high-accuracy optomechanical parts of various non-imaging optical systems. The increased accuracy of the manufacturing of complex-shaped mechanical parts has also led to the possibility of using the CNC machining in the reformation of the optomechanics for the imaging optical systems. The high-accuracy of the CNC machined optomechanical parts among with the fluent data transfer between the optical and mechanical design programs and the computer aided manufacture (CAM) gives a lot of freedom for the optical design.

We have designed and manufactured a 2.7 times de-magnifying imaging optical system (see Figure 1) capable of resolving features smaller than $5\ \mu\text{m}$ in the image plane. The specification of the lens is shown in Table 1. The optical system is a double-telecentric catadioptric system consisting of the total of 13 optical elements: 9 lenses, 1 mirror, 2 polarising beam splitters and 1 quarter wave plate (Figure 2). The numerical aperture (NA) is 0.18 on the object side and 0.44 on the image side. The distortion of the lens is less than 0.01 %. The field size is 23 mm in diameter on the object side and 8.6 mm in the image side. The measured modulation transfer function (MTF) of the system is over 34 % at 200 linepairs/mm (see Figure 3).

Table 1. Specification of the lens

Magnification	0.37	0.37
Image size (diagonal)	8.5 mm	8.5
Object NA	> 0.15	0.18
Image NA	≥ 0.41	0.44
Distortion	< 0.03 %	< 0.01 %
MTF @ 200 lp/mm	60 %	> 34 %
Wavelength	$405 \pm 10\ \text{nm}$	$405 \pm 10\ \text{nm}$

The optomechanics are composed of 2 larger pieces and several smaller parts; all of the parts are made using the 5-axis CNC machining. One of the larger pieces provides a 90 degree angle in the optical path with less than 0.5' accuracy. The overall accuracy of the mechanics is 0.01 mm and the dimensions are 300 mm x 150 mm x 70 mm. The tolerances for the optical and mechanical components were determined via optical simulations. The performance predicted by the tolerance analysis is shown as a set of MTF curves in Figure 3. The measured MTF

shown in Figure 3 is clearly below the predicted MTF values. The measurement was, however, done without a sheet of glass covering the object plane, and thus the measured MTF can be considered as a worst-case estimate. The influence of the missing cover glass was analysed with optical simulations and the estimated performance with the cover glass on is shown as the dashed line in Figure 3. The optomechanical design also included the stray light analysis (see Figure 4) resulting some minor modifications to the mechanical parts. The realised lens is shown in Figure 5.

Because of the use of the high-accuracy CNC machining of the optomechanics, the lens can be manufactured without any optical adjustments or testing in the assembly phase.

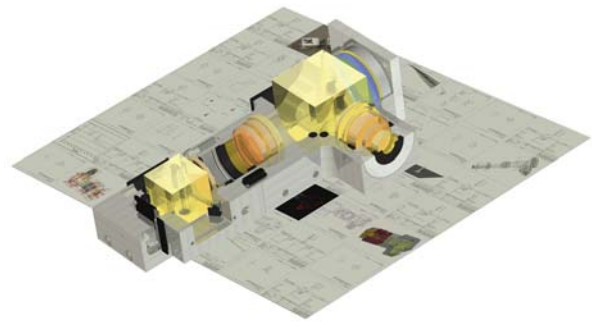


Figure 1: Optical and mechanical 3-D modelling combined with CMC machining enables design and manufacturing of high resolution optics needing no optical adjustments.

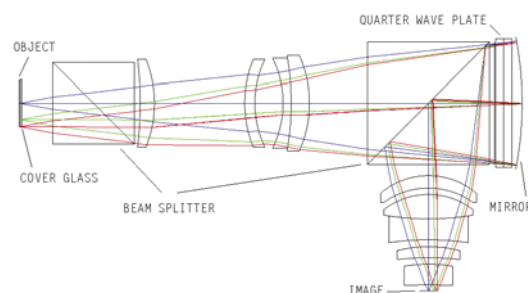


Figure 2: The optical design of the imaging lens.

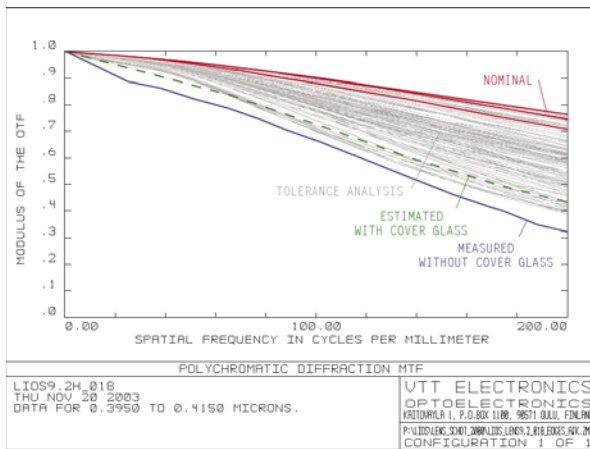


Figure 3: Modulation transfer function of the designed optical system. The result of the tolerance analysis is based on 20 Monte Carlo runs. Due to mechanical limitations in MTF measurement system, the MTF curve was measured without the cover glass on top of the object plane. The optical simulation predicted, that this fault drops the MTF from the nominal design by 10 percentage units.

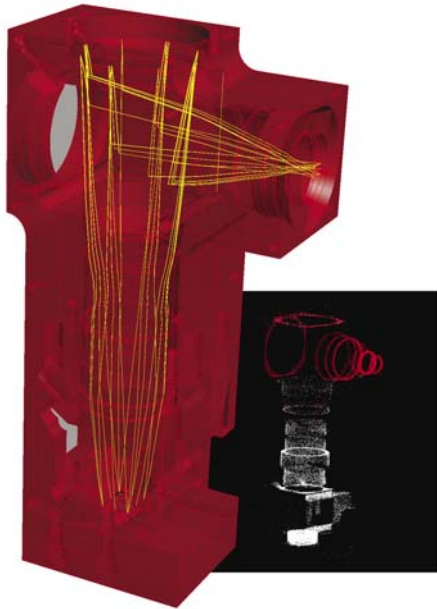


Figure 4: The stray light analysis was used for fine-tuning the optomechanics. The optomechanical model is shown on the left side of the figure. A stray-light simulation result is shown on the right side. White dots illustrate the mechanical surfaces seen from the object plane (and thereby potentially illuminated with the stray light) whereas the red dots indicate the surfaces seen from the image plane. The stray light on the image plane is significantly decreased by eliminating the surfaces that can be seen from both the image and the object planes.

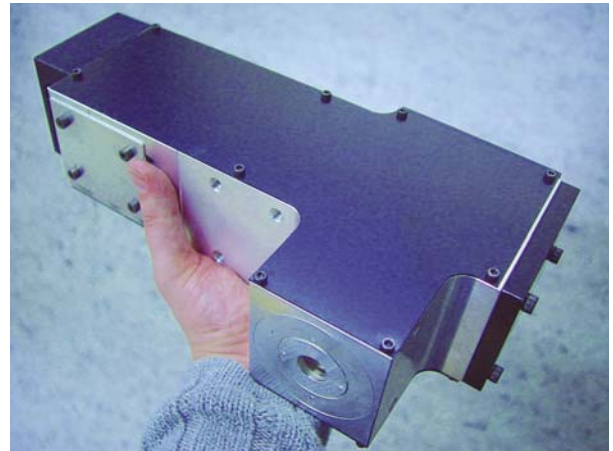


Figure 5: A photograph of the realised lens.



Janne Aikio
Janne.Aikio@vtt.fi



Pekka Suopajarvi
Pekka.Suopajarvi@vtt.fi



Tapio Seppänen
Tapio.Seppanen@vtt.fi



Mauri Aikio
Mauri.Aikio@vtt.fi

C. Edström
M. Tannemyr
Beacon AB, Förrådsvägen 10, SE-901 32, Umeå, Sweden

H. Vasama
Suomen Optomekaniikka, Jokelantie 1 40270 Palokka, Finland